Skin type and nerve effects on cortical tactile processing: a somatosensory evoked potentials study

Marco Guidotti, Clément Beaurieux, Pierre Marionnaud, Frédérique Bonnet-Brilhault, Claire Wardak, Marianne Latinus

Skin type and nerve effects on cortical tactile processing: a somatosensory evoked potentials study

Marco Guidotti[a,b,c], Clément Beaurieux[a], Pierre Marionnaud[a], Frédérique Bonnet-Brilhault[a,b], Claire Wardak[a,#], Marianne Latinus[a,#]

[a] : UMR 1253, iBrain, Université de Tours, Inserm, Tours, France

[b] : EXcellence Center in Autism and neurodevelopmental disorders-Tours, Centre Universitaire de Pédopsychiatrie, CHRU de Tours, Tours, France

[c] : Centre Hospitalier du Chinonais, Saint-Benoît-la-Forêt, France

co-last authors

Abbreviated title: **Skin type and nerve effects in SEP**

Corresponding author:

Claire Wardak
claire.wardak@univ-tours.fr
ORCID : https://orcid.org/0000-0001-8847-1859
CHRU de Tours - UMR 1253 Imagerie et Cerveau
2, Bd Tonnellé – 37000 Tours (France)

New & Noteworthy

The current paper highlights the influence of stimulated skin type (glabrous/hairy) and nerve (median/radial) on cortical somatosensory evoked potentials. Mechanical stimulations were applied over four territories of the right hand in 18 adults. Four middle latency components were identified: P50, N80, N130 and P200. A larger N80 was found after glabrous skin stimulations than after hairy skin ones, regardless of the nerve being stimulated. P50 and N80 were larger after median than radial nerve stimulations.

Abstract

Somatosensory evoked potentials (SEP) studies typically characterize short latency components following median nerve stimulations of the wrist. However, these studies rarely considered 1) skin type (glabrous/hairy) at the stimulation site, 2) nerve being stimulated, and 3) middle latency (>30 ms) components. Our aim was to investigate middle latency SEPs following simple mechanical stimulation of two skin types innervated by two different nerves. Eighteen adults received 400 mechanical stimulations over four territories of the right hand (two nerves: radial/median; two skin types: hairy/glabrous skin) while their EEG was recorded. Four middle latency components were identified: P50, N80, N130 and P200. As expected, significantly shorter latencies and larger amplitudes were found over the contralateral hemisphere for all components. A skin type effect was found for the N80: glabrous skin stimulations induced larger amplitude than hairy skin stimulations. Regarding nerve effects, median stimulations induced larger P50 and N80. Latency of the N80 was longer after median nerve stimulation than radial nerve stimulation. This study showed that skin type and stimulated nerve influence middle latency SEPs, highlighting the importance of considering these parameters in future studies. These modulations could reflect differences in cutaneous receptors and somatotopy. Middle latency SEPs can be used to evaluate the different steps of tactile information cortical processing.

Significance: Modulation of SEPs components before 100 milliseconds possibly reflects somatotopy and differential processing in primary somatosensory (SI) cortex.

Keywords: glabrous skin, SEP, median nerve, radial nerve

1. Introduction

Tactile processing is a complex phenomenon and many of its facets are still unknown. Somatosensory evoked potentials (SEPs) can be used to characterize the time-course and processing steps of tactile information. They are often studied in clinical investigations to explore the integrity of the ascending peripheral pathways (1), therefore focusing on very early SEPs components. SEPs can also be useful to better describe cortical processing of tactile information, with a very interesting temporal definition despite a limited spatial resolution (2). SEPs are modulated by several factors, like nerve type, skin type, location and type of stimulation, although their direct influence has not systematically been quantified.

SEPs are usually recorded after electrical stimulation of the median nerve, the most accessible nerve in the upper limb, which conveys both motor and sensory information. The superficial branch of the radial nerve, which is purely sensory, has also been explored, and smaller SEPs component amplitudes are described (3,4). Most studies focus on short latency potentials, with several components usually described in adults during the first 20 ms and generated in peripheral structures: P8/P9 from the brachial plexus (5–7), P11 from the dorsal columns of the cervical spinal cord (5,6) and P12/P13, whose generator is probably located in the brainstem lemniscus (5–7). Initial subcortical processing begins around 14 ms (P14), with a thalamic response identified at 16 ms (N16); thalamocortical radiations generate a contralateral N20 peak, also called N1 (5–10). Between 20 and 60 ms, activation of primary somatosensory cortex is observed through the P30/N45 and the P50/N60 complexes, originating, respectively, from Brodmann area 3b and 1 (11–14). After these early components, middle-latency SEPs can be observed; yet studies are heterogeneous and results are divergent. Tactile pulses and vibratory stimuli evoke several contralateral and ipsilateral responses. First, a negative deflection (N70/N80) is generally found over central and posterior electrodes (14–16). A second positive peak is described bilaterally, at ~100 ms (P100), originating from secondary somatosensory cortex (SII) (14–17). The P100 is followed by a negative component, the N125/N140, generated in SII and modulated by attention (14–16,18). A positive peak is then recorded at 200 ms (P200) and may be generated in the lateral surface of SII (14,19,20). Contrary to short-latency SEPs, the influence of the nerve being stimulated has never been explored for middle-latency SEPs.

The location of the tactile stimulation also impacts SEPs. The wrist, a hairy skin territory, and the fingertip, in glabrous skin, are both targeted to study SEPs following median nerve stimulation (5,7,15,21). Both glabrous and hairy skins convey discriminative touch information, although via low-threshold myelinated afferents connected to only partially overlapping receptor types (22–24). In glabrous skin (palm of the hand), four types of mechanoreceptors units are described: two slowly adapting types (Merkel cells and Ruffini endings) and two rapidly adapting types (Meissner and Pacinian corpuscles) (25). In hairy skin, at least 5 types of low-threshold mechanoreceptive afferent have been identified: two slowly adapting (SA) units (Merkel cells - SAI and maybe Ruffini endings – SAII) and three rapidly adapting (RA) units (hair-, field- and Pacinian-types) (24,26). Meissner corpuscles are absent of hairy skin territory. The density of mechanoreceptors is generally lower in hairy than in glabrous skin (26). Furthermore, unmyelinated C-tactile afferents were also identified in the skin (27–29), mostly in hairy territories (30–32). These fibers convey affective touch information to the brain and are poorly sensitive to vibratory stimuli (23,33–37). To our knowledge, no study has directly compared SEPs resulting from glabrous or hairy skin stimulation of the same nerve, although they might differ considering the differences in mechanoreceptors between these two types of skin.

SEPs are also sensitive to the type of stimulation used, with most studies relying on electrical stimulations that directly excite the fibers, hence yielding clear SEPs (1,38). However, this non-natural stimulation does not allow to obtain SEPs comparable to those observed after mechanical stimulations (39,40) or to target specific fiber types. Mechanical stimulations are vibratory stimulation with varying frequencies from very low (unique indentation) to high frequency (e.g., textures are transmitted by complex vibrations). Vibratory stimulations may allow to target specific fiber types, as each type of mechanosensory fiber is more sensitive to a specific range of vibratory frequencies depending of the intensity of the stimulation: SAI and SAII respond well to low frequencies, RAI and RAII are more easily excited at high frequencies (above 8 Hz, and 64 Hz, respectively), but can also respond to lower frequencies at higher intensity of stimulation (41,42). In this study, we focused on short unique mechanical stimulations, probably activating all mechanoreceptive afferents, to evoke cortical SEPs.

In light of all these factors, we wanted to systematically evaluate the influence of two factors on middle latency SEPs: nerve type and skin type. Specifically, we aimed at evaluating if the SEPs pattern usually described following median nerve stimulation was found after radial nerve

stimulation. For each nerve, we also evaluated how skin type (glabrous or hairy) influenced somatosensory cortical processing. Finally, to the best of our knowledge the influence of the nerve stimulated on cortical processing (e.g., on middle latency SEPs) of touch has not been evaluated, we therefore focused on middle latency SEPs. We expected larger SEPs after median nerve stimulations than after radial ones, and after stimulation of glabrous skin compared to hairy one, in particular for components generated in primary and secondary somatosensory cortex (e.g. up to 80 ms).

2. Methods

2.1. Participants

Twenty-two adults were included in this study. Exclusion criteria were: evidence of central nervous system disease, sensory deficit, epilepsy, brain or head injury, psychiatric disorder, and difficulties in motor, language or learning development. Data of four participants were excluded because of an insufficient number of trials after artifacts rejection. The final group included 18 adults aged 20 to 32 (mean age in years ± standard deviation: 23.2 ± 2.7, 9 males, 9 females). No difference was found in age between male and female groups (p = 0.102). Informed written consent was obtained from all adult participants. The study was approved by an ethics committee (CPP n° 2017-A00756-47; Clinical Trial NCT03182400) and all procedures were conducted according to the principles of the Declaration of Helsinki.

2.2. Procedure

During EEG recordings, the subjects were sitting in a reclining armchair located 70 cm away from a computer screen. Subjects watched a black cross on a gray background presented on the screen during the experiment. Tactile stimuli were delivered by four vibrotactile electromagnetic solenoid-type stimulators (Tactors, Dancer Design) attached to the skin with adhesive rings and adhesive plasters. These 18mm diameter cylindrical tactors delivered a 50-ms single stimulation on a 4-mm diameter circular surface, with an estimated force of 0.35N. We did not test a vibrotactile stimulation, only the initial mechanical stimulation by the pin inside the solenoid. Hairy and glabrous skin areas were targeted in two different territories of the radial and median nerves of the right hand (Fig. 1): the back (site 4) and palm side (site 3) tip of the middle finger, and the back (site 2) and palm side (side 1) of the lateral part of the

thenar eminence. Stimulation sites were chosen to best test our hypothesis, that is to disentangle nerve and skin type effects; however, it is noteworthy that site 1 (palm side of the thenar eminence) and 4 (dorsum side of the tip of middle finger) are border sites that could be innervated by multiple nerves depending on the individuals.

Two stimulation blocks were tested, separated by a short break. Each block was composed of 240 single stimuli (60 per location, 4 locations), delivered in a randomized order, for a total duration of 12 minutes. In each block, the inter-stimuli interval (ISI) was variable, between 1,000 and 1,885 ms for 50 trials per location (short ISI trials, mean: 1,264 ms) and between 10,000 and 11,220 ms for 10 trials (long ISI trials, mean: 10,348 ms) per location. Only short ISI trials were considered for analysis (100 trials per location).

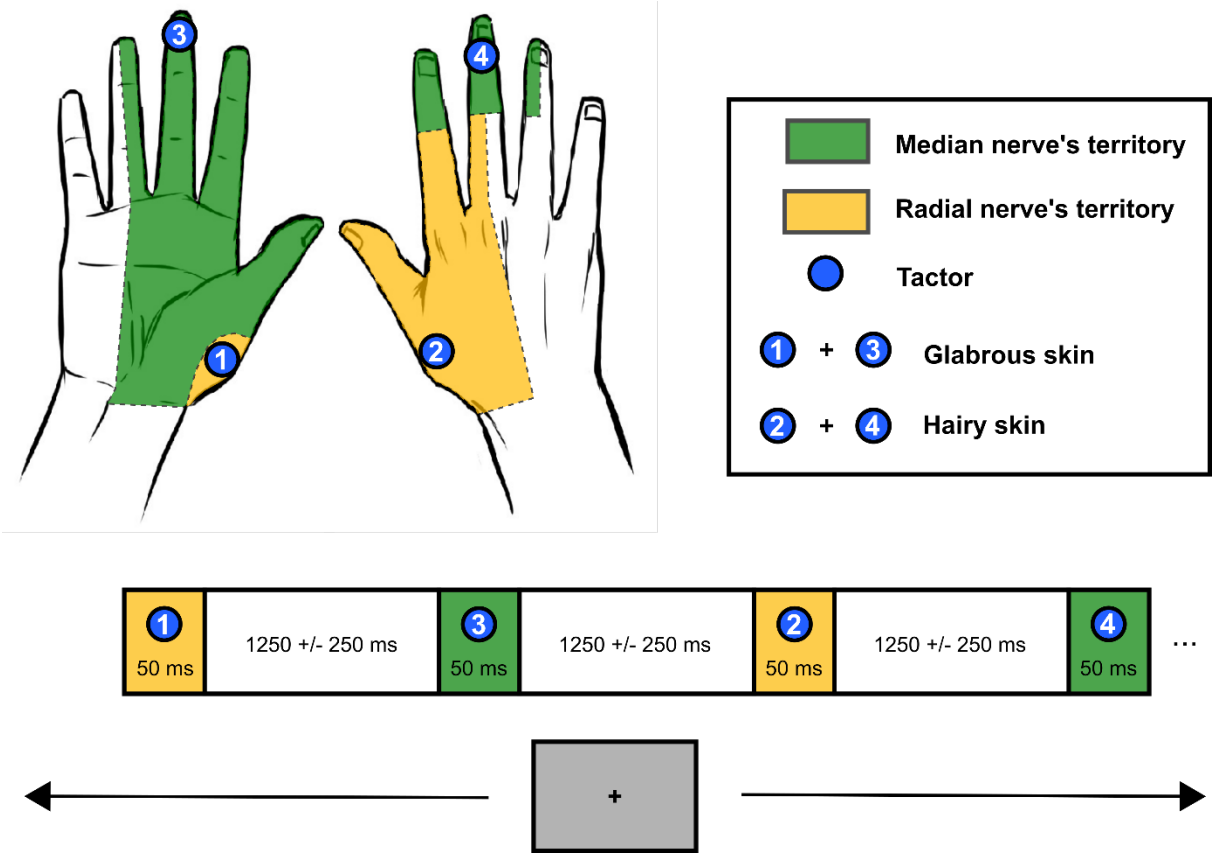

Figure 1: Territories targeted by tactile mechanical stimulations and experimental procedure. Tactile stimuli were delivered on the right hand by four vibrotactile stimulators. Hairy and glabrous skin areas were targeted in the radial and median nerve territories. Sixty stimulations per location per block were delivered, with a variable inter-stimuli interval (1,250ms +/-250 ms for 50 trials and 11,000 ms +/- 1,000 ms for 10 trials). Subjects watched a black cross on a gray background presented on the screen during the experiment.

2.3. EEG recording and pre-processing

A 64-channel ActiveTwo system (Biosemi, The Netherlands) was used for EEG recording. Electrodes placed at the outer canthi of the eyes and below the left eye allowed to monitor blinks and saccades; an external electrode was placed on the tip of the nose to allow offline referencing to the nose if needed. The signal was recorded at a sampling frequency of 1,024 Hz and filtered at 0–100 Hz. A 0.1 Hz digital high-pass filter was applied to the EEG signal. Bad channels were identified by visual inspection. Ocular artifacts were corrected by applying an independent component analysis (ICA; without bad channels) on the continuous EEG signal as implemented in EEGLab (43) running in Matlab (The Mathworks, Inc). Blink artifacts were captured into components that were automatically removed via the inverse ICA transformation. After components removal, bad channels were interpolated, and data were re-referenced to an average reference. Continuous EEG signal was time-locked to trial onset; trials were extracted between −100 ms pre-stimulus and 800 ms post-stimulus. Baseline correction (−100 to 0 ms) was applied. After creating epochs around the stimulation, trials containing artifacts (e.g., with muscle activity or movements) were rejected based on visual inspection of the signal. ERPs were computed by averaging all trials of a condition leading to 4 ERPs per subject: Median-Hairy (number of trials (mean ± s.d.): 78±18); Median-Glabrous (77.8±17.8); Radial-Hairy (78±16.4); Radial-Glabrous (76.3±17.7). ERPs were digitally filtered with a low-pass frequency cut-off of 40 Hz.

2.4. Data analysis

The identification of middle-latency components was performed by averaging the data for all subjects and conditions. Electrodes and time intervals were selected based on the exploration of grand averages (collapsed across nerve and skin types) using both topographies and time courses. First, we looked at time courses to identify the evoked components, then we looked at topographies at the peak of each component to identify electrodes of interests. In all subjects and for all conditions, four components were identified between 25 and 500ms after the beginning of the tactile stimulation: P50, N80, N130 and P200 (Fig. 2 and 3). Peak latency and amplitude were measured on the average ERPs of each subject. P50 was measured as the maximum positive deflection in the 25-65 ms time window over centroparietal electrodes (C3/C4, C5/C6, CP1/CP2, CP3/CP4, CP5/CP6). N80 was measured as the maximum negative deflection between 60 and 100 ms over C3/C4, C5/C6. N130 was measured as the maximum

negativity over FC5/FC6, C5/C6 in the 100-150 ms time window and finally P200 was the maximum positive deflection measured between 160 ms and 240 ms over FC1/FC2, C1/C2, FCz/Cz. Note that the time window used for measurements was not completely respected when measuring P50 in the ipsilateral hemisphere due to the inconsistent responses recorded over ipsilateral electrodes.

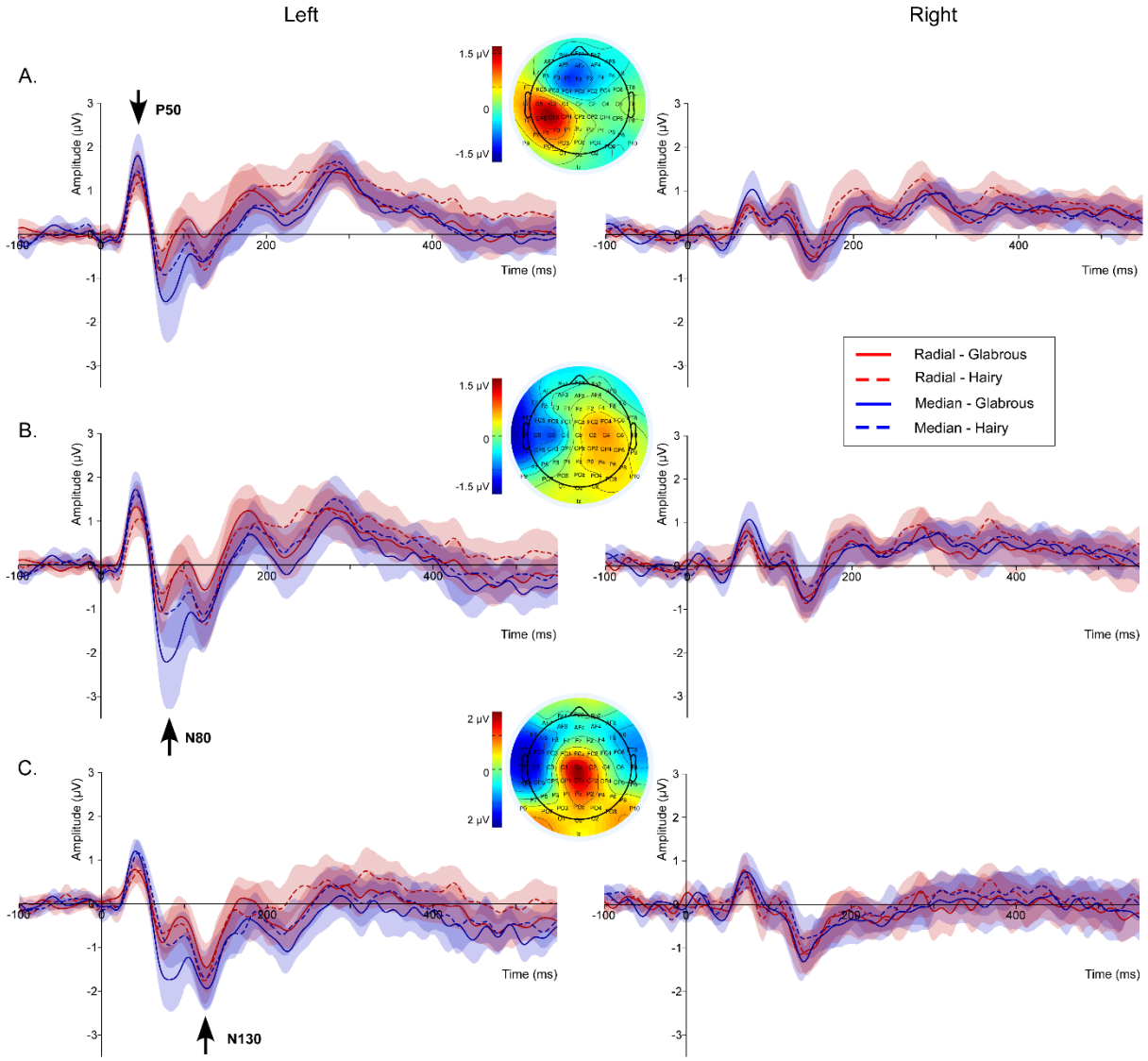

Figure 2: Somatosensory evoked potential (SEP)s' middle-latency components for the four different conditions. (A) The P50 component is presented for the left and right hemispheres. The left P50 was recorded in C3, C5, CP1, CP3 and CP5, and the right P50 in C4, C6, CP2, CP4 and CP6. For each condition (red: radial nerve; blue: median nerve; solid line: glabrous skin; dashed line: hairy skin), the average of the selected electrodes (colored line) and 95% CI (shaded area) are presented. The central inset represents the topography of all conditions at 50 ms. (B) The N80 component is presented for the left and right hemispheres. The left N80 was recorded in C3 and C5 and the right N80 in C4 and C6. The central inset represents the topography of all conditions at 80 ms. Same conventions as in (A). (C) The N130 component is presented for the left and right hemispheres. The left N130 was recorded in FC5 and C5 and the right N130 in FC6 and C6. The central inset represents the topography of all conditions at 127 ms. Same conventions as in (A).

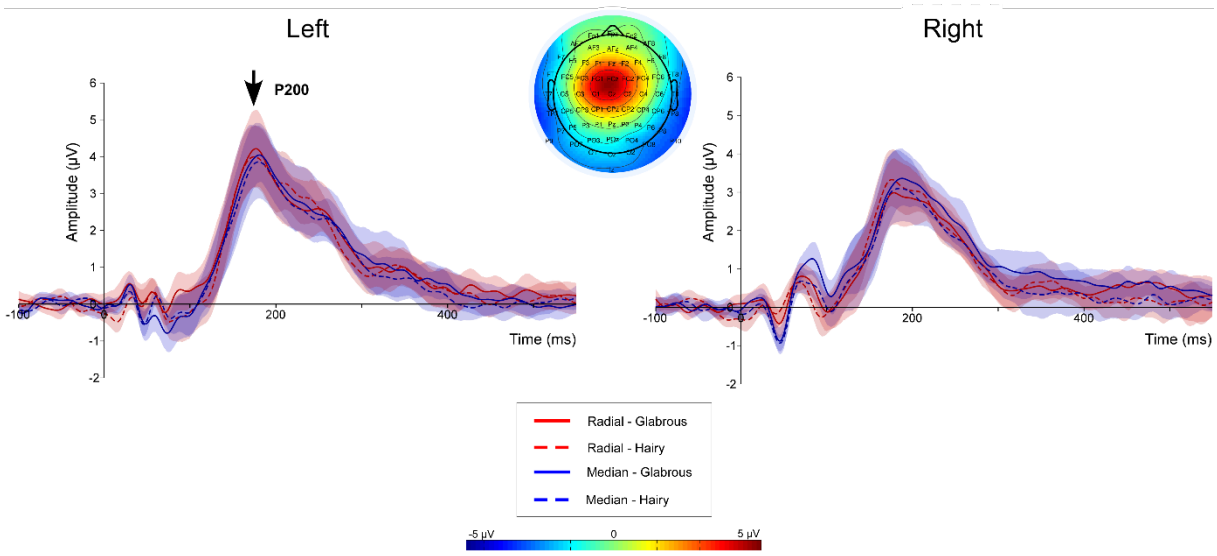

Figure 3: P200 component in the left and right hemispheres for the four different conditions. The left component was recorded in FC1 and C1, the right component in FC2 and C2. The central inset represents the topography of all conditions at 180 ms. Same conventions as in Fig. 2.

Statistical analyses and graphs were done in R desktop v1.4.1717 (RStudio, PBC, Boston, MA) using the following packages: *tidyverse* (44), *rstatix* (45), *ggplot2* (46), *ggpubr* (47) and *gridExtra* (48). Two repeated-measure analysis of variance (ANOVA) were carried out for each component. First, to evaluate lateralization of components, ANOVA with hemisphere, nerve and skin as within-subject factors were conducted on data averaged across electrodes. Second, due to a predominant contralateral response, ANOVA with electrodes, nerve and skin as within-subject factors were conducted on data from the left hemisphere only. First, gender was included as a between-subject factor in the ANOVA; due to lack of significant effects, a second ANOVA was run without sex.

Interaction between nerve and electrodes on the P50 was further investigated using a *t* test (collapsed across skin type) at each time point and electrode. To estimate statistical significance of the *t* test we built a data-driven distribution of *t* values under the null hypothesis of a lack of difference between median and radial nerve stimulations. Data was permuted across conditions for each participant independently after data centering. Random permutations were repeated 5,000 times. We stored *t* and *p* values after each permutation for each time point and electrode separately. To correct for multiple comparisons, we performed a two-dimensional (2D) spatial-temporal clustering using the result of the 5,000 resampling as implemented in LIMO EEG (48).

F, *t* and *p* values are provided, as well as effect sizes. Significance was considered for $p < 0.05$.

3. Results

3.1. Hemisphere effect

Hemisphere effects were found for all middle-latency components (Fig. 4). SEPs recorded during the first 100 ms were essentially found in electrodes located over the left hemisphere, contralateral to the tactile stimulation. After 100 ms, SEPs were progressively more central, with a more bilateral response.

P50 latency was significantly shorter in the contralateral (left) compared to the ipsilateral (right) hemisphere (44.05 +/- 5.69 ms vs. 61.42 +/- 17.59 ms; $F(1,17) = 28.180$; $p < 0.001$; ges = 0.316). Its amplitude was significantly larger in the left hemisphere (1.65 +/- 1.12 µV) than in the right one (0.86 +/- 0.84 µV; $F(1,17) = 27.045$; $p < 0.001$; ges = 0.150).

For the N80, latency was significantly shorter in the left hemisphere (77.80 +/- 9.73 ms) compared to the right hemisphere (86.54 +/- 14.99 ms; $F(1,17) = 13.513$; $p < 0.01$; ges = 0.115). Its amplitude was larger in the contralateral (left) than in the ipsilateral (right) hemisphere (-2.04 +/- 2.16 µV vs –0.14 +/- 0.91 µV; $F(1,17) = 20.875$; $p < 0.001$; ges = 0.230).

Significantly shorter latency and larger amplitude were also found in the left hemisphere compared to the right hemisphere for the N130 (latency: 126.26 +/- 10.67 ms vs 136.03 +/- 14.52 ms; $F(1,17) = 10.904$; $p < 0.01$; ges = 0.130; amplitude: -2.03 +/- 1.28 µV vs –1.34 +/- 1.27 µV, $F(1,17) = 4.927$; $p < 0.05$; ges = 0.095) and the P200 (latency: 188.90 +/- 23.51 ms vs 195.75+/- 21.57 ms; $F(1,17) = 5.581$; $p < 0.05$; ges = 0.023; amplitude: 4.55 +/- 2.14 µV vs 3.71 +/- 1.83 µV; $F(1,17) = 11.099$; $p < 0.01$; ges = 0.054).

3.2. Skin and nerve effects in the left hemisphere

Figure 4 summarizes skin and nerve effects recorded in the left contralateral hemisphere for all components. Only the significant findings are presented in the text; the overall results are summarized in Table 1.

P50

A significant nerve effect was observed for the contralateral P50: the amplitude after median nerve stimulation was larger (1.33 +/- 1.17 µV) than after radial nerve stimulation (1.18 +/- 0.94 µV; $F(1,17) = 5.946$; $p < 0.05$; ges = 0.027).

An electrode effect was found, linked to a nerve by electrode interaction for this component ($F(2,41) = 3.729$; $p = 0.026$). Pairwise comparisons showed amplitude differences between

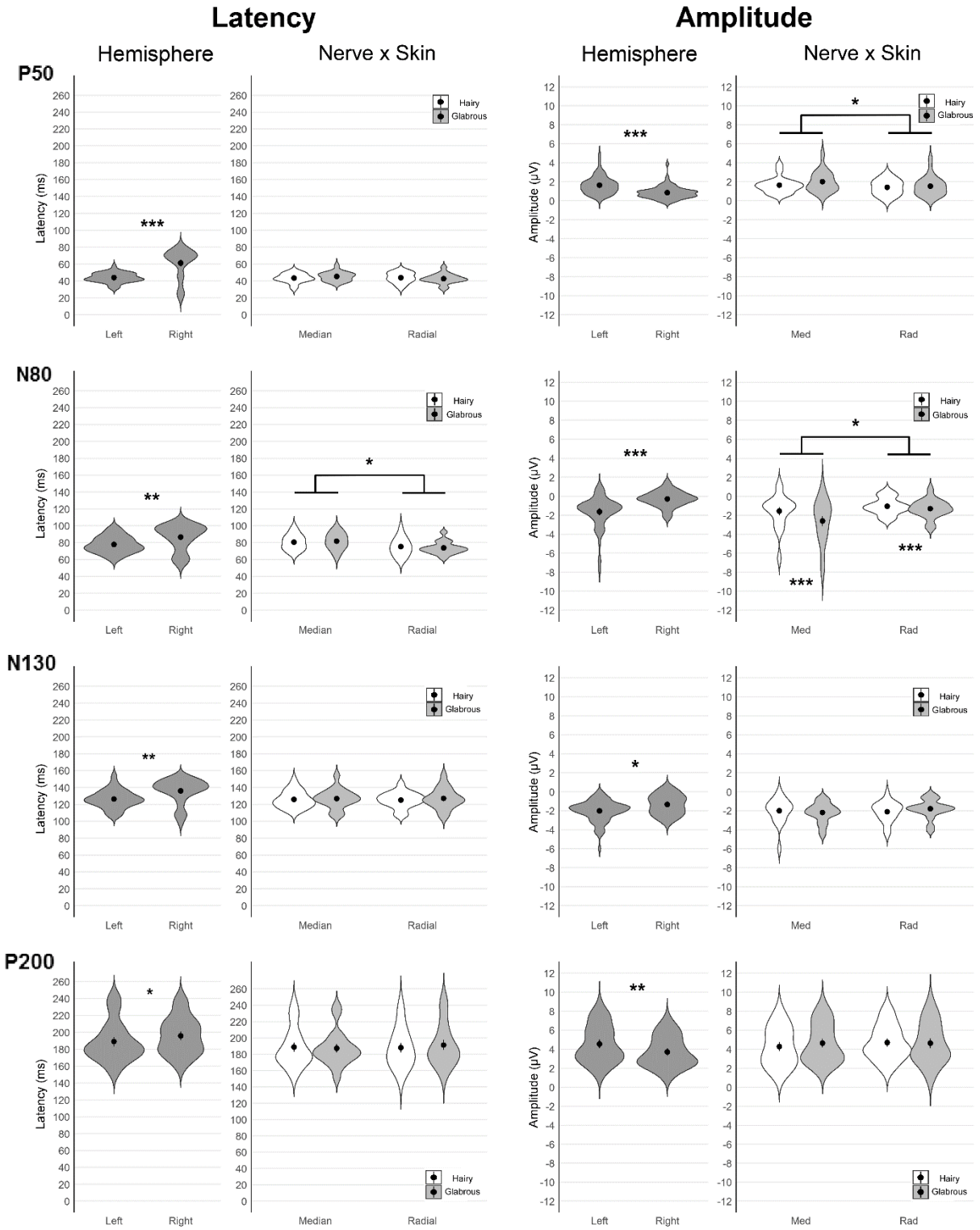

Figure 4: Hemisphere, nerve and skin effects on the latency and amplitude of P50, N80, N130 and P200 components. The latency effects are presented on the left, the amplitude on the right. For each parameter, the left column corresponds to the hemisphere effect and the right column to the skin and nerve effects within the contralateral hemisphere. Data distributions are represented by violin plots (dark gray: hemisphere; light gray: glabrous skin (i.e., low-CT territories); white: hairy skin (i.e., high-CT territories)) and mean scores +/- SE by black points and lines. * $p < 0.05$; ** $p < 0.01$; *** $p < 0.001$.

Component	Latency			Amplitude		
	Nerve effect	Skin effect	Skin by Nerve Interaction	Nerve effect	Skin effect	Interactions
P50	F(1,17) = 0.774; p = 0.391	F(1,17) = 0.129; p = 0.724	F(1,17) = 2.286; p = 0.149	**F(1,17) = 5.946; p < 0.05; ges = 0.027**	F(1,17) = 3.9; p = 0.065	**NxE: F(2,41) = 3.729; p = 0.026** SxE: F(3,44) = 0.825; p = 0.473 SxN: F(1,17) = 0.731; p = 0.404 SxNxE: F(1.56, 26.5) = 1.983; p = 0.165
N80	**F(1,17) = 8.266; p < 0.05; ges = 0.122**	F(1,17) = 0.007; p = 0.936	F(1,17) = 0.903; p = 0.355	**F(1,17) = 6.336; p < 0.05; ges = 0.071**	**F(17) = 15.898; p < 0.001; ges = 0.038**	NxE: F(1,17) = 0.764; p = 0.394 SxE: F(1,17) =0.007; p = 0.937 SxN: F(1,17) = 4.054; p = 0.060 SxNxE: F(1,17) = 0.009; p = 0.924
N130	F(1,17) = 0.005; p = 0.946	F(1,17) = 0.481; p = 0.497	F(1,17) = 0.140 ; p = 0.713	F(1,17) = 0.824; p = 0.377	F(1,17) = 0.280; p = 0.604	NxE: F(1,17) = 0.318; p = 0.58 SxE: F(1,17) = 11.318; p = 0.81 SxN: F(1,17) = 2.606; p = 0.125 SxNxE: F(1,17) = 2.396; p = 0.14
P200	F(1,17) = 0.116; p = 0.738	F(1,17) = 0.086; p = 0.772	F(1,17) = 0.468; p = 0.503	F(1,17) = 1.166; p = 0.295	F(1,17) = 1.055; p = 0.319	NxE: F(1,17) = 1.034; p = 0.324 SxE: F(1,17) = 0.006; p = 0.939 SxN: F(1,17) = 1.879; p = 0.188 SxNxE: F(1,17) = 0.016; p = 0.889

Table 1: Summary of skin, nerve, and interaction effects on latency and amplitude for all components recorded in the contralateral (left) hemisphere. N: Nerve; S: Skin; E: Electrode. x in SxE, for instance, means interaction. Significant effects are highlighted in bold.

radian and median nerve stimulations on C5 (p < 0.01), and between CP1 and the other electrodes for median nerve stimulation (CP1 vs. C3: p = 0.020; CP1 vs. C5: p = 0.023; CP1 vs. CP3: p < 0.001; CP1 vs CP5: p < 0.001) and between CP1 and CP3 following radial nerve stimulation (p < 0.001). To further investigate this interaction, we performed t tests at each time point and electrodes between 24 and 65 ms. This analysis revealed significant differences in the topographies observed for median and radial nerves (Fig. 5), starting as early as 33 ms and up to 64 ms after stimulation. Significant differences were observed over fronto-central electrodes and frontotemporal electrodes, likely highlighting differences in the source of the P50 after

stimulation of the radial and median nerves. Activations observed after median nerve stimulation were more medial than after stimulation of the radial nerve (Fig. 5).

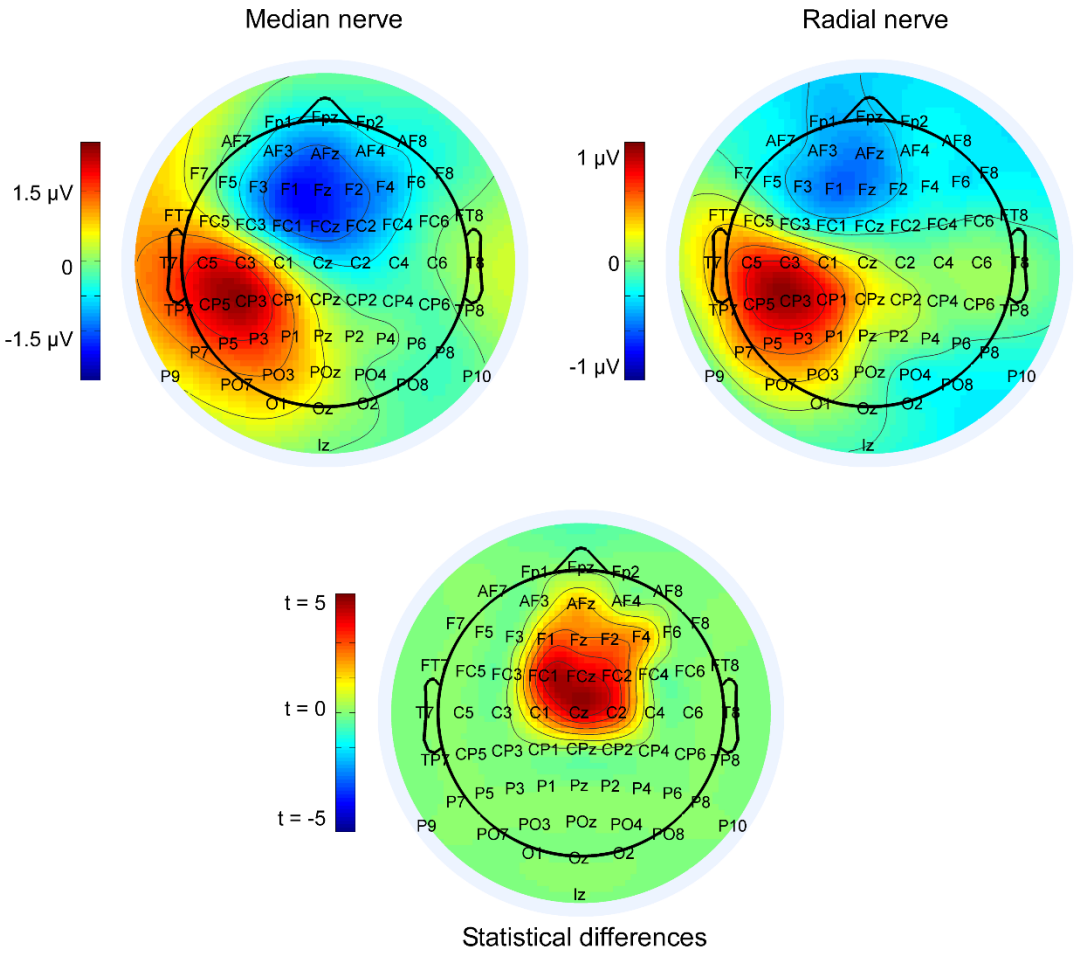

Figure 5: Topographies at 50 ms. Top: Topographies of evoked activity following median and radial nerves stimulations. Bottom: Topography of significant *t* values, after spatial-temporal clustering correction for multiple comparisons. Non-significant values are in green.

N80

A significant nerve effect was observed for the contralateral N80, both for latency and amplitude. N80 latency was shorter after radial nerve stimulation compared to median nerve stimulation (81.33 ± 13.15 ms vs. 86.88 ± 12.61 ms; $F(1,17) = 8.266$; $p < 0.05$; ges = 0.122). N80 amplitude was larger after median nerve stimulation (-1.14 +/- 1.93 µV) than after radial nerve's one (–0.76 +/- 1.08 µV; $F(1,17) = 6.336$; $p < 0.05$; ges = 0.071).

Furthermore, the amplitude of the N80 was larger after stimulation of the glabrous skin than after stimulation of the hairy skin (–1.07 +/- 1.78 µV vs -0.83 +/- 1.34 µV; $F(17) = 15.898$; $p < 0.001$; ges = 0.038).

N130

No significant effect was found for this component.

P200

No significant effect was found for this component.

4. Discussion

Our original study identified four middle-latency SEP components and determined the modulatory effects of skin type and nerve being stimulated on somatosensory cortical processing, something rarely done. We found an important skin effect on the N80 and nerve effects on the P50 and the N80.

In our study, components obtained after mechanical stimulations mostly confirmed findings from previous works using different kind of stimulations (15,19,50,51). Note that studies that compared different types of stimulations, mainly electrical and mechanical stimulations, reported contradictory results with either earlier (between 2 and 10 ms, depending on the component; 39) or later (between 4 and 6 ms, depending on the component; 40) SEPs for mechanical stimulations. All recorded SEPs were larger in the contralateral hemisphere. Consistent with previous reports, middle-latency components up to 80 ms were mainly observed in sites contralateral to the stimulation (52) and reflect processing in somatosensory cortex SI (50). However, the precise origin of P50 and N80 is not clearly established, with mainly contribution of area 1 for P50 and possibly contributions of both areas 1 and 3b for N80 (50). After 100 ms, recordings were less lateralized, although responses remained earlier and larger in the left hemisphere, with localization closer to the midline. We hypothesize that SEPs after 100 ms (N130 and P200 in our study), probably involving the SII cortex (14,19,20), represent important steps in the integration of tactile information, more independent from body side (53) and low-level information, as they were not sensitive to the nerve or skin type being stimulated.

We found that skin type affected only one component: the N80 was larger after glabrous skin stimulations than hairy skin ones. The P50 does not seem sensitive to skin type, however, statistics revealed a marginal effect of skin type: glabrous skin stimulation evoked slightly larger P50 than hairy skin stimulation. Our protocol did not allow the observation of earlier components, which origin is better defined (11,14), preventing us to definitively conclude on

the origin of our skin type effect. Either P50 and N80 are sensitive to skin type, and we lack power to properly establish it for P50, or the differential contribution of areas 1 and 3b in these components (11,14,50) explain that only N80 is sensitive to skin type. Skin types differ in mechanoreceptor types and density and in peripheral and central receptive fields' sizes. Indeed, we know that glabrous skin has a higher density of mechanoreceptors than the hairy skin (24,26,41), and some mechanoreceptors in the hairy skin have very large receptive fields (26). Neurons of area 3b have small receptive fields (54) and are mainly responsive to low-level stimulus properties (orientation, speed of movement and stimulus rate) (55). Therefore, we can suppose that the skin type effect on the N80 reflects a higher density of Aβ afferents in glabrous skin which in turns activate more neurons in area 3b, one of the putative source of the N80 (50) but not of P50.

Nerve effects were observed on early middle-latency SEPs components, mainly P50 and N80. Amplitudes of the P50 and the N80 were larger after median than radial nerve stimulation, consistent with our hypothesis. This amplitude difference is in line with the results of Treede and Kunde (56) and those of Grisolia and Wiederholt (4) on early SEPs, and probably reflects two phenomena, independent of stimulus intensity which was constant in our study. First, the median nerve territory possesses a higher density of sensitive mechanoreceptive units and Aβ fibers, especially in distal parts of fingers (25,31,32). This could lead to the recruitment of a greater number of receptors during median nerve stimulation, and then a greater number of neurons in the SI and SII cortex. Second, the nature of the nerve stimulated may also alter SEPs (3,4). Indeed, the median nerve contains sensory and motor fibers, unlike the superficial radial nerve, which is entirely sensory. The larger median nerve SEPs could likely results from these two phenomena (57).

A significant nerv-by-electrode interaction was found for the P50. This could reflect different somatotopy in SI cortex between median and radial nerves territories. Significant differences in topographies suggest a different cortical representation of median nerve territory, which would be more lateral, compared to radial nerve territory, more medial (Fig. 5). Even if our 64-channel EEG system is not dense enough to precisely document this spatial difference, this result is consistent with hand and index surfaces described on the sensory homunculus (58-60).

We found an earlier N80 after stimulation of the radial nerve than after the median nerve. This is more difficult to interpret, in particular with respects to the lack of latency differences on the P50. Previous studies on very early SEPs after electrical stimulations of the wrist reported

contradictory results either no differences (3,4), later (56) or earlier SEPs (56,57) for median nerve stimulations. We chose our stimulation sites close enough to limit a possible difference in conduction distance between the stimulator and the cortical generators. However, there is still a 15-to-20 cm distance between the sites of stimulation for the two nerves. In addition, radial and median nerve differ in terms of conduction velocity, with the radial nerve being faster than the median nerve at least between the fingers and the wrist (61,62). Note however, that conduction velocity recorded from the forearm may be similar for radial and median nerve. Differences in distance between stimulation sites combined with differences in velocity can explain a difference of ~5 ms between radial and median nerve stimulations. Yet, conduction velocity could be expected to modulate earlier components, although in our study P50 latency was not modulated by nerve. We hypothesize that as the P50 represents mainly the activity of area 1 which processes more integrated information and lies at a higher processing stage than 3b (63), it is less sensitive to the body part being stimulated. On the other hand, area 3b which is involved in the processing of low-level information (55) and contributes mainly to N80 could be more sensitive to stimulation location. The latency difference on the N80 seems thus to reflect the combinatory effect of different peripheral conduction velocity, distance and central processing (56).

We did not find any skin-by-nerve interaction. This lack of effect could reflect the high individual variability in the exact innervation of sites 1 and 4. Indeed, sites 1 and 4 are close to the border of the radial and median nerve territories, respectively, and could, in some individuals, comprise different types of nerves.

To conclude, middle-latency SEPs, elicited by mechanical non-social stimulations, were influenced by skin types and nerves stimulated, suggesting the importance of taking skin type and the nerve being stimulated into account for any SEPs exploration, in order to better interpret each result. The different middle latency SEPs components appears to arise from different brain regions, in link with different steps of tactile information processing and could help us better understand tactile perception.

Conflict of Interest Statement: None of the authors have potential conflicts of interest to be disclosed.

Funding Source: None.

5. Bibliography

1. Cruccu G, Aminoff MJ, Curio G, Guerit JM, Kakigi R, Mauguiere F, et al. Recommendations for the clinical use of somatosensory-evoked potentials. Clin Neurophysiol. 2008 Aug 1;119(8):1705–19.

2. Picton TW, Bentin S, Berg P, Donchin E, Hillyard SA, Johnson R, et al. Guidelines for using human event-related potentials to study cognition: Recording standards and publication criteria. Psychophysiology. 2000 Mar;37(2):127–52.

3. Fujii M, Yamada T, Aihara M, Kokubun Y, Noguchi Y, Matsubara M, et al. The effects of stimulus rates upon median, ulnar and radial nerve somatosensory evoked potentials. Electroencephalogr Clin Neurophysiol. 1994 Nov;92(6):518–26.

4. Grisolia JS, Wiederholt WC. Short latency somatosensory evoked potentials from radial, median and ulnar nerve stimulation in man. Electroencephalogr Clin Neurophysiol. 1980 Dec;50(5–6):375–81.

5. Anziska BJ, Cracco RQ. Short latency SEPs to median nerve stimulation: comparison of recording methods and origin of components. Electroencephalogr Clin Neurophysiol. 1981 Dec;52(6):531–9.

6. Gilmore R. Use of somatosensory evoked potentials in infants and children. Neurol Clin. 1988 Nov;6(4):839–59.

7. Tsuji S, Shibasaki H, Kato M, Kuroiwa Y, Shima F. Subcortical, thalamic and cortical somatosensory evoked potentials to median nerve stimulation. Electroencephalogr Clin Neurophysiol. 1984 Nov;59(6):465–76.

8. Yamada T, Kayamori R, Kimura J, Beck DO. Topography of somatosensory evoked potentials after stimulation of the median nerve. Electroencephalogr Clin Neurophysiol. 1984 Feb;59(1):29–43.

9. Gobbelé R, Waberski TD, Simon H, Peters E, Klostermann F, Curio G, et al. Different origins of low- and high-frequency components (600 Hz) of human somatosensory evoked potentials. Clin Neurophysiol. 2004 Apr 1;115(4):927–37.

10. Jung P, Baumgärtner U, Bauermann T, Magerl W, Gawehn J, Stoeter P, et al. Asymmetry in the human primary somatosensory cortex and handedness. NeuroImage. 2003 Jul 1;19(3):913–23.

11. Allison T, Wood CC, McCarthy G, Spencer DD. Cortical somatosensory evoked potentials. II. Effects of excision of somatosensory or motor cortex in humans and monkeys. J Neurophysiol 1991 Jul 1; 66:64-82.

12. Jung P, Baumgärtner U, Magerl W, Treede RD. Hemispheric asymmetry of hand representation in human primary somatosensory cortex and handedness. Clin Neurophysiol. 2008 Nov 1;119(11):2579–86.

13. Allison T. Scalp and Cortical Recordings of Initial Somatosensory Cortex Activity to Median Nerve Stimulation in Man. Ann N Y Acad Sci. 1982;388(1):671–8.

14. Allison T, McCarthy G, Wood CC, Williamson PD, Spencer DD. Human cortical potentials evoked by stimulation of the median nerve. II. Cytoarchitectonic areas generating long-latency activity. J Neurophysiol. 1989 Sep 1; 62:711-722.

15. Hämäläinen H, Kekoni J, Sams M, Reinikainen K, Näätänen R. Human somatosensory evoked potentials to mechanical pulses and vibration: contributions of SI and SII somatosensory cortices to P50 and P100 components. Electroencephalogr Clin Neurophysiol. 1990 Feb;75(2):13–21.

16. Eimer M, Forster B. Modulations of early somatosensory ERP components by transient and sustained spatial attention. Exp Brain Res. 2003 Jul;151(1):24–31.

17. Frot M, Mauguière F. Timing and spatial distribution of somatosensory responses recorded in the upper bank of the sylvian fissure (SII area) in humans. Cereb Cortex N Y N 1991. 1999 Dec;9(8):854–63.

18. Hoechstetter K, Rupp A, Meinck HM, Weckesser D, Bornfleth H, Stippich C, et al. Magnetic source imaging of tactile input shows task-independent attention effects in SII. NeuroReport. 2000 Aug 3;11(11):2461.

19. Frot M, Rambaud L, Guénot M, Mauguière F. Intracortical recordings of early pain-related CO2-laser evoked potentials in the human second somatosensory (SII) area. Clin Neurophysiol Off J Int Fed Clin Neurophysiol. 1999 Jan;110(1):133–45.

20. Frot M, Garcia-Larrea L, Guénot M, Mauguière F. Responses of the supra-sylvian (SII) cortex in humans to painful and innocuous stimuli. A study using intra-cerebral recordings. Pain. 2001 Oct;94(1):65–73.

21. Montoya P, Sitges C, García-Herrera M, Izquierdo R, Truyols M, Blay N, et al. Abnormal affective modulation of somatosensory brain processing among patients with fibromyalgia. Psychosom Med. 2005;67(6):957–63.

22. Handler A, Ginty DD. The Mechanosensory Neurons of Touch and their Mechanisms of Activation. Nat Rev Neurosci. 2021 Sep;22(9):521–37.

23. McGlone F, Wessberg J, Olausson H. Discriminative and affective touch: sensing and feeling. Neuron. 2014 May 21;82(4):737–55.

24. Abraira VE, Ginty DD. The Sensory Neurons of Touch. Neuron. 2013 Aug 21;79(4):10.1016/j.neuron.2013.07.051.

25. Johansson RS, Vallbo AB. Tactile sensibility in the human hand: relative and absolute densities of four types of mechanoreceptive units in glabrous skin. J Physiol. 1979 Jan;286:283–300.

26. Vallbo AB, Olausson H, Wessberg J, Kakuda N. Receptive field characteristics of tactile units with myelinated afferents in hairy skin of human subjects. J Physiol. 1995 Mar 15;483 (Pt 3):783–95.

27. Vallbo A, Olausson H, Wessberg J, Norrsell U. A system of unmyelinated afferents for innocuous mechanoreception in the human skin. Brain Res. 1993 Nov 19;628(1–2):301–4.

28. Olausson H, Wessberg J, Morrison I, McGlone F, Vallbo A. The neurophysiology of unmyelinated tactile afferents. Neurosci Biobehav Rev. 2010 Feb;34(2):185–91.

29. Löken LS, Wessberg J, Morrison I, McGlone F, Olausson H. Coding of pleasant touch by unmyelinated afferents in humans. Nat Neurosci. 2009 May;12(5):547–8.

30. McGlone F, Olausson H, Boyle JA, Jones-Gotman M, Dancer C, Guest S, et al. Touching and feeling: differences in pleasant touch processing between glabrous and hairy skin in humans. Eur J Neurosci. 2012 Jun 1;35(11):1782–8.

31. Wessberg J, Olausson H, Fernström KW, Vallbo ÅB. Receptive Field Properties of Unmyelinated Tactile Afferents in the Human Skin. J Neurophysiol. 2003 Mar 1;89(3):1567–75.

32. Watkins RH, Dione M, Ackerley R, Backlund Wasling H, Wessberg J, Löken LS. Evidence for sparse C-tactile afferent innervation of glabrous human hand skin. J Neurophysiol. 2020 Dec 9;125(1):232–7.

33. Cascio CJ, Moore D, McGlone F. Social touch and human development. Dev Cogn Neurosci. 2019;35:5–11.

34. Morrison I, Löken LS, Olausson H. The skin as a social organ. Exp Brain Res. 2010 Jul 1;204(3):305–14.

35. Ackerley R, Backlund Wasling H, Liljencrantz J, Olausson H, Johnson RD, Wessberg J. Human C-tactile afferents are tuned to the temperature of a skin-stroking caress. J Neurosci Off J Soc Neurosci. 2014 Feb 19;34(8):2879–83.

36. Olausson H, Lamarre Y, Backlund H, Morin C, Wallin BG, Starck G, et al. Unmyelinated tactile afferents signal touch and project to insular cortex. Nat Neurosci. 2002 Sep;5(9):900–4.

37. Ackerley R. C-tactile (CT) afferents: evidence of their function from microneurography studies in humans. Curr Opin Behav Sci. 2022 Feb 1;43:95–100.

38. Aminoff MJ, Eisen AA. AAEM minimonograph 19: Somatosensory evoked potentials. Muscle Nerve. 1998;21(3):277–90.

39. Yamauchi N, Fujitani Y, Oikawa T. Somatosensory evoked potentials elicited by mechanical and electrical stimulation of each single pain or tactile spot of the skin. Tohoku J Exp Med. 1981 Jan;133(1):81–92.

40. Kakigi R, Shibasaki H. Scalp topography of mechanically and electrically evoked somatosensory potentials in man. Electroencephalogr Clin Neurophysiol. 1984 Feb;59(1):44–56.

41. Johansson RS, Landström U, Lundström R. Responses of mechanoreceptive afferent units in the glabrous skin of the human hand to sinusoidal skin displacements. Brain Res. 1982 Jul 22;244(1):17–25.

42. Mountcastle VB, LaMotte RH, Carli G. Detection thresholds for stimuli in humans and monkeys: comparison with threshold events in mechanoreceptive afferent nerve fibers innervating the monkey hand. J Neurophysiol. 1972 Jan;35(1):122–36.

43. Delorme A, Makeig S. EEGLAB: an open-source toolbox for analysis of single-trial EEG dynamics. J Neurosci Methods 134: 9-21, 2004.

44. Wickham H, Averick M, Bryan J, Chang W, McGowan L, François R, et al. Welcome to the Tidyverse. J Open Source Softw. 2019 Nov 21;4:1686.

45. Alboukadel K. rstatix: Pipe-Friendly Framework for Basic Statistical Tests. 2021; Available from: https://CRAN.R-project.org/package=rstatix

46. Wickham H. ggplot2: Elegant Graphics for Data Analysis. Springer; 2016. 266 p.

47. Kassambara A. ggpubr: "ggplot2" Based Publication Ready Plots. 2020. Available from: https://CRAN.R-project.org/package=ggpubr

48. Auguie B, Antonov A. gridExtra: Miscellaneous Functions for "Grid" Graphics. 2017 Available from: https://CRAN.R-project.org/package=gridExtra

49. Pernet CR, Chauveau N, Gaspar C, Rousselet GA. LIMO EEG: a toolbox for hierarchical LInear MOdeling of ElectroEncephaloGraphic data. Comput Intell Neurosci. 2011;2011:831409.

50. Allison T, McCarthy G, Wood CC. The relationship between human long-latency somatosensory evoked potentials recorded from the cortical surface and from the scalp. Electroencephalogr Clin Neurophysiol. 1992 Aug;84(4):301–14.

51. Yamada H, Yaguchi H, Tomatsu S, Takei T, Oya T, Seki K. Representation of Afferent Signals from Forearm Muscle and Cutaneous Nerves in the Primary Somatosensory Cortex of the Macaque Monkey. PLOS ONE. 2016 Oct 4;11(10):e0163948.

52. Yamada T. Somatosensory Evoked Potentials. In: Aminoff MJ, Daroff RB, editors. Encyclopedia of the Neurological Sciences (Second Edition). Oxford: Academic Press; 2014. p. 230–8.

53. Tamè L, Braun C, Lingnau A, Schwarzbach J, Demarchi G, Li Hegner Y, et al. The contribution of primary and secondary somatosensory cortices to the representation of body parts and body sides: an fMRI adaptation study. J Cogn Neurosci. 2012 Dec;24(12):2306–20.

54. DiCarlo JJ, Johnson KO, Hsiao SS. Structure of Receptive Fields in Area 3b of Primary Somatosensory Cortex in the Alert Monkey. J Neurosci. 1998 Apr 1;18(7):2626–45.

55. Hlushchuk Y, Simões-Franklin C, Nangini C, Hari R. Stimulus-Rate Sensitivity Discerns Area 3b of the Human Primary Somatosensory Cortex. PLoS ONE. 2015 May 28;10(5):e0128462.

56. Treede RD, Kunde V. Middle-latency somatosensory evoked potentials after stimulation of the radial and median nerves: component structure and scalp topography. J Clin Neurophysiol Off Publ Am Electroencephalogr Soc. 1995 May;12(3):291–301.

57. Koivikko MJ. Differences in evoked potentials to median and radial nerve stimulation in man. Brain Res. 1971 Jul 9;30(1):223–7.

58. Roux F, Djidjeli I, Durand J. Functional architecture of the somatosensory homunculus detected by electrostimulation. J Physiol. 2018 Mar 1;596(5):941–56.

59. Sun F, Zhang G, Ren L, Yu T, Ren Z, Gao R, et al. Functional organization of the human primary somatosensory cortex: A stereo-electroencephalography study. Clin Neurophysiol Off J Int Fed Clin Neurophysiol. 2021;132(2):487–97.

60. Schellekens W, Thio M, Badde S, Winawer J, Ramsey N, Petridou N. A touch of hierarchy: population receptive fields reveal fingertip integration in Brodmann areas in human primary somatosensory cortex. Brain Struct Funct. 2021;226(7):2099–112.

61. Choi KC, Hah JS, Byun YJ, Park CS, Yang CH. A Study of Nerve Conduction Velocity of Normal Adults. J Yeungnam Med Sci. 1989 Jun 30;6(1):151–63.

62. Hirata M, Sakakibara H. Sensory nerve conduction velocities of median, ulnar and radial nerves in patients with vibration syndrome. Int Arch Occup Environ Health. 2007 Feb;80(4):273–80.

63. Hsiao S. Central mechanisms of tactile shape perception. Curr Opin Neurobiol. 2008 Aug 1;18(4):418–24.